# Fano-like resonance phenomena by flexural shell modes in sound transmission through two-dimensional periodic arrays of thin-walled hollow cylinders

Yuriy A. Kosevich,[1,*] Cecile Goffaux,[2,†] and Jose Sánchez-Dehesa[1,‡]

[1]*Wave Phenomena Group, Nanophotonics Technology Center, Polytechnic University of Valencia, C/Camino de Vera s/n, E-46022 Valencia, Spain*

[2]*CENAERO, 30 Avenue Jean Mermoz, B-6041 Gosselies, Belgium*

(Received 28 February 2006; published 12 July 2006)

It is shown that the $n=2$ and 3 flexural shell vibration modes of thin-walled hollow cylinders result in Fano-like resonant enhancement of sound wave transmission through or reflection from two-dimensional periodic arrays of these cylinders in air. The frequencies of the resonant modes are well described by the analytical theory of flexural (circumferential) modes of thin-walled hollow cylinders and are confirmed by finite-difference time-domain simulations. When the modes are located in the band gaps of the phononic crystal, an enhancement of the band-gap widths is produced by the additional restoring forces caused by the flexural shell deformations. Our conclusions provide an alternative method for the vibration control of airborne phononic crystals.

DOI: 10.1103/PhysRevB.74.012301 PACS number(s): 62.30.+d, 46.40.−f

Periodic arrays of elastic scatterers in air, which have acoustic band gaps in the audible frequency range, are called phononic or sonic crystals (SCs).[1] Such artificial airborne composite systems can be used for shielding sound waves within given frequency ranges in a controllable manner. A typical example of a SC is a two-dimensional (2D) array of solid cylinders in air. Because of very high contrast between density and sound velocity in air and in ordinary solids, like metals, the transmission properties of 2D SCs, made of complete (or thick-walled hollow) cylinders in air, almost do not depend on the elastic properties of the cylinders.[2] The reason is that the eigenfrequencies of elastic vibrations of solid cylinders are much higher than characteristic frequencies of the lowest acoustic band gap (BG) in the SC, $\sim\tilde{c}\pi/a$, where $\tilde{c}$ is the effective sound velocity of the order of (or lower than) sound velocity in air.[3–5] But this situation can be drastically changed in the case of 2D SCs made of *thin-walled* hollow cylinders. The point is that cylinders with the wall thickness $d$ much less than the radius $r$ have flexural shell vibrations at very low frequencies.[6,7] These frequencies can be located in the BGs of the SC, by the proper choice of the $d/r$ ratio and elastic properties of the cylinder material.

If the transmission coefficient of sound waves through the elastic shell is designed to be not very small, the sound vibration can resonantly excite the corresponding flexural shell vibration, which results in resonant enhancement of sound transmission through or reflection from the SC. This resonance has in general the asymmetric line shape typical for the Fano resonance[8] because there are two possible paths for the wave transmission through the array of cylinders: via the flexural shell vibration mode and via the background continuum of vibrational states. The interference between these two paths produces the asymmetric Fano-like line shape of the signal transmitted through the finite-thickness SC. The asymmetric line shape of the transmission coefficient, namely the enhanced transmission followed by the enhanced reflection at the higher frequency, was reported in connection with various kinds of localized resonances.[9–12]

In this paper, we study analytically and numerically the transmission properties of sonic crystals made of 2D arrays of thin-walled hollow cylinders in air using the finite-difference time-domain (FDTD) method. In comparison with corresponding SCs made of complete (or thick-walled hollow) cylinders, the transmission properties of this new composite medium present two main physical features: (i) strong Fano-like resonances appear in the transmission spectra, and (ii) the width of the BG increases with increasing filling fraction of thin-walled hollow cylinders in the SC. Analytical expressions for the resonance frequencies are presented and a physical picture of both phenomena is discussed.

As is known from the theory of vibration of shells, the flexural (circumferential) and radial modes of a shell are coupled and the dispersion equation for their frequencies in the limit of an infinitely long cylinder can be written in the following form:[6,7,13]

$$\Omega^4 - \Omega^2[1 + n^2 + \alpha(n^2 - 1)^2] + \alpha n^2(n^2 - 1)^2 = 0, \qquad (1)$$

where $\Omega^2 = 4\pi^2\rho_s(1-\sigma_s^2)r^2\nu^2/E_s$; $\alpha = d^2/(12r^2)$; $\rho_s$, $E_s$, and $\sigma_s$ are, respectively, the density, Young modulus, and Poisson ratio of the solid; and $n=0,1,2,\ldots$ is the circumferential mode number. Frequencies of the flexural and radial shell vibration modes are given, respectively, by the lower and higher solutions of Eq. (1). For thin-walled shells with $\alpha \ll 1$ and for not very high mode number $n$, Eq. (1) gives the following expression for the frequency of the $n$th flexural shell vibration mode of a solid hollow cylinder with $\sigma_s=1/3$:

$$\nu_n = \frac{n(n^2-1)}{\sqrt{1+n^2}}\frac{d}{r^2}\frac{C_{ts}}{4\pi}, \qquad (2)$$

where $C_{ts}$ is the transverse elastic wave velocity in cylinder material. For the given Poisson ratio of the solid, the longitudinal elastic wave velocity $C_{ls}=2C_{ts}$. As follows from Eq. (2), the lowest flexural shell vibration mode corresponds to $n=2$. Frequencies of flexural shell modes increase linearly with thickness $d$, are inverse to $r^2$, and increase with $n$ approximately as $n^2$. Such modes can be supported only by

 

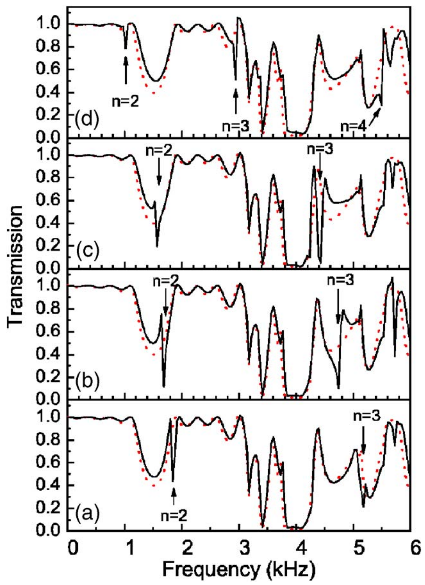


FIG. 1. (Color online) Transmission spectra through four-layer SC of square symmetry with period $a=11$ cm of complete (red dotted lines) and hollow (black solid lines) cylinders with $r=2$ cm. (a), (b), (c), and (d) correspond, respectively, to shell thicknesses $d=2.0$, 1.9, 1.8, and 1.2 mm. The arrows indicate the positions of the transmission or reflection resonances related with the $n=2$, 3, and 4 flexural shell modes.

solid shells since their frequencies are determined by the velocity of the transverse wave in the material $C_{ts}$.

In order to achieve substantial interaction between a sound wave in air and the $n$th flexural shell vibration mode of the hollow cylinder, we require that the coefficient of intensity transmission $T$ of a sound wave with linear frequency $\nu_n$, normally incident from air on the shell with thickness $d$, should be (approximately) more than 0.1. The coefficient of intensity transmission through the thin planar layer with thickness $d$ can be written as[14]

$$T=\frac{1}{1+\left(\frac{\pi\nu_n d\rho_s}{\rho_a C_{la}}\right)^2}, \tag{3}$$

where $\rho_a$ and $C_{la}=340$ m/s are the density and sound velocity in air. It is assumed in Eq. (3) that $2\pi\nu_n d/C_{ls}\ll 1$ and there is a strong acoustic mismatch between air and solid, $Z_a\ll Z_s$, where $Z_i=\rho_i C_{li}$ are acoustic impedances for longitudinal waves in air and solid, $i=a,s$. We use Eq. (3) in the following for the estimate of the transmission coefficient through the shells of thin-walled solid cylinders. The aforementioned requirement on the transmission coefficient $T$ imposes, via the mode frequency $\nu_n$ given by Eq. (2), rather severe restrictions on the radius and thickness of thin-walled hollow cylinders and on sound velocity and density of their material.

Figure 1 presents FDTD calculations of the transmission spectra through four-layer airborne SCs of square symmetry with lattice constant $a=11$ cm. Spectra corresponding to structures made of thin-walled hollow cylinders (black solid lines) with different shell thickness are compared with the spectrum of the SC made of complete cylinders (red dashed lines). The filling fraction $f$ $(=\pi r^2/a^2)$ of the corresponding 2D lattice is 0.10. We assume that the slabs have infinite extensions along the lateral $(y)$ and vertical $(z)$ directions. The sound is incident along the normal $(x)$ direction to the slab. Both $x$ and $y$ axes are parallel to the sides of the square unit cell of the SC. In the calculations, the discretization mesh in real space is chosen to be $\Delta x=\Delta y=a/400$, whereas $N=2^{19}$ steps of time were taken into account with $\Delta t=0.25\Delta x/C_{ls}\sqrt{2}$. For the acoustic properties of the material of solid cylinders, we use $\rho_s=0.050$ g/cm$^3$, or $\rho_s=50\rho_a$, $C_{ts}=2000$ m/s, $C_{ls}=4000$ m/s. These parameters are artificially chosen and they correspond to an extraordinary light material with sound velocities of metals such as brass or bronze. However, materials such as aerogels or those made of carbon nanotubes accomplish these requirements. These parameters allow us to excite the $n=2$ flexural shell mode at the midgap of the first stopband of SC made of a 2D array of thin-walled hollow cylinders with $d=1.9$ and 1.8 mm, see Figs. 1(b) and 1(c), which is possible due to the relatively high transmission coefficient of the correspoding sonic vibration through the shell, $T=0.34$ in Eq. (3). As is seen from Figs. 1(b) and 1(c), this mode results in Fano-like resonance enhancement of the transmission coefficient in the forbidden frequency range (band gap) around 1.5 kHz.

Further analysis of Fig. 1 reveals the presence of the higher modes in the transmission spectra through four-layer SCs, composed from thin-walled cylinders, around 4.5 kHz, Figs. 1(a)–1(c), and around 3 and 5.5 kHz, Fig. 1(d). We relate these resonances with the $n=3$ and 4 flexural shell vibration modes (see also below).

Another important phenomenon occurs when the resonance modes are located in phonon passbands; see Fig. 1(a) for the $n=2$ mode, Fig. 1(c) for the $n=3$ mode, and Fig. 1(d) for the $n=2$ and 3 modes. In this case, the resonance results in a strong reflection from the SC that is characterized by a minimum in the transmission spectrum. Therefore, the flexural shell vibration modes can produce two different effects. There is a resonance enhancement of sound transmittance through the SC when the modes are located on the *low* background density of vibrational states in phonon band gaps, see also Fig. 2 below, while there is a resonance enhancement of sound reflectance from the SC when the modes are located on tbe *high* background density of vibrational states in phonon passbands. The characteristic asymmetric line shape of both the transmission and reflection resonances, in the band gaps and passbands, respectively, clearly reveals the interference Fano-like origin of these resonances. This property of 2D SCs made of thin-walled hollow cylinders can be used to design acoustic metamaterials based on SCs.

In Fig. 2, we plot FDTD calculations of the transmission spectrum through four-layer airborne SCs composed from the same 2D system of complete (red dashed lines) and hollow (black solid lines) cylinders with $d=2$ mm shell thickness as described in Fig. 1, but with $a=5.5$ cm lattice period. In this case, $f=0.41$. For the acoustic properties of the material of solid cylinders, we use $\rho_s=0.017$ g/cm$^3$, or $\rho_s=17\rho_a$, $C_{ts}=4000$ m/s, $C_{ls}=8000$ m/s. These parameters ensure the high transmission of sound through a cylinder

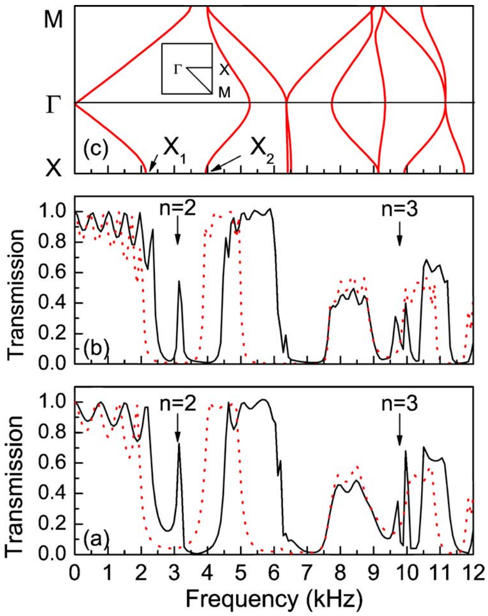


FIG. 2. (Color online) Transmission spectra through four-layer (a) and six-layer (b) SC of square symmetry with period $a$=5.5 cm. Red dotted lines show the spectra of SC made of complete cylinders, while black solid lines show the ones corresponding to hollow cylinders with radius $r$=2 and shell thickness $d$=2.0 mm. The arrows indicate the positions of transmission resonance related with the $n$=2 and 3 flexural shell modes. (c) Phononic band structure along the two high-symmetry directions (see inset) in SC of complete cylinders with the same period and filling fraction.

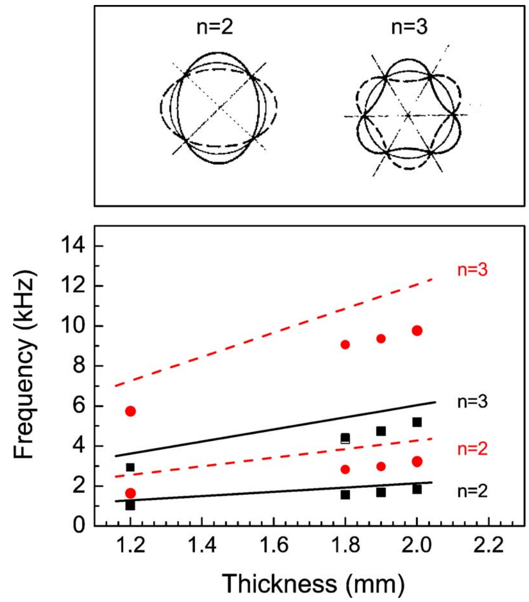


FIG. 3. (Color online) Lower panel: Frequency positions vs shell thickness of the analytically predicted [see Eq. (2)] flexural shell vibration modes (lines) and numerically revealed transmission/reflection resonances (symbols). Solid and dashed lines correspond to the shells with $C_{ts}$=2000 and 4000 m/s, respectively. Upper panel: Eigenmode deformation of a hollow cylinder associated with the $n$=2 and 3 flexural shell modes.

shell at the midgap of the first stopband; $T$=0.53 at $\nu_2 \approx 3$ kHz. For the $n$=2 modes, the comparison of Figs. 1 and 2 shows that the asymmetric Fano-like shape of the resonance transmission is suppressed with an increasing filling fraction $f$. The Fano-like shape is also suppressed with an increasing number of layers for a given $f$, cf. Figs. 2(a) and 2(b). In other words, the Fano resonance is replaced by a regular resonant transmission with almost symmetric line shape.[9] This effect is caused by the decreasing background density of vibrational states. The transmission minima for the slabs of complete cylinders [dashed lines in Figs. 2(a) and 2(b)] correspond to the band gaps (pseudogaps) in the phonon bands along the Γ$X$ direction in 2D SC of complete cylinders, shown in Fig. 2(c). In Fig. 2(c), the phonon bands along the Γ$M$ direction are also shown, which define the full band gap of this sonic crystal.

In Fig. 3, we plot frequency positions of the flexural shell vibration modes (lines) analytically predicted by Eq. (2) and numerically revealed transmission/reflection resonances (symbols) versus shell thickness $d$. The better agreement between the analytical formula in Eq. (2) and FDTD numerical simulations is reached for the SC with the lower $f$, which corresponds to the case of cylinders with $C_{ts}$=2000 m/s, because the flexural shell vibration mode in each cylinder is less affected by the interaction with neighbor cylinders in the SC with lower filling fraction. From this figure we can conclude that the enhanced band-gap transmission or enhanced passband reflection can indeed be related with the excitation of flexural shell modes in hollow cylinders by sound vibration in SC. These findings also explain the physical origin and give analytical expression for the frequencies of previously numerically revealed tunable narrow passbands inside the first BG in a 2D composite medium made of a square array of steel hollow cylinders embedded in water.[15,16]

From Fig. 2, we can also see that there are upward shifts of both edges of the first BG in the hollow cylinder SC. Also, there is a corresponding shift of the transmission maxima (Fabry-Perot oscillations) in the first phonon band. Both effects can be related with the increase of the effective sound velocity in a thin-walled cylinder SC with respect to that in the complete cylinder SC. The latter, in turn, can be related with the high transparency of thin walls of the cylinders, which makes air in the interior and exterior of the cylinders strongly dynamically coupled. The decrease of sound velocity in complete cylinder SCs is determined by the filling fraction of the SC, $\tilde{c}=C_{la}/\sqrt{1+f}$,[3,4] and $f$=0.41 for SCs with $r$=2 cm and $a$=5.5 cm, while the effective filling fraction of thin-walled cylinder SCs should be close to zero because of strong "cross-talk" between the interior and exterior of the cylinders. This explains why the ratio of effective sound velocities in thin-walled and complete cylinder SCs, which one can extract from the Fabry-Perot oscillations in the first phonon band in Fig. 2, is close to $\sqrt{1+f}$=1.19. It is worth mentioning that this property of effective sound velocity, caused by the effective filling fraction, can also be applied to sound velocity in porous silicon aerogels since the latter can be considered as composite media made of thin-walled silicon nanostructures in air.

To understand the upward shift of the upper edge of the first BG in thin-walled cylinder SCs, in Fig. 4 we plot the

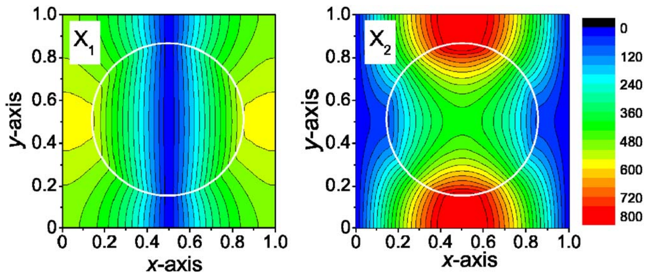


FIG. 4. (Color online) Modulus of the pressure distribution associated with the bottom ($X_1$) and upper ($X_2$) modes of the first pseudogap [see Fig. 2(c)]. They are plotted in a unit cell.

modulus of the pressure distribution for the bottom ($X_1$) and upper ($X_2$) modes of the first BG in a unit cell of complete cylinder SCs [see Fig. 2(c)]. As follows from the comparison of Figs. 3 and 4, the pressure distribution at the upper edge ($X_2$) of the first BG has the symmetry of the $n=2$ mode and therefore causes flexural deformation of cylinders. The latter results in the additional restoring forces, caused by cylinder flexural rigidity, which shift upward the upper edge of the BG in thin-walled cylinder SC. This upward shift increases with the cylinder filling fraction due to relative increase of the cylinder surface within each unit cell of the SC, which is clearly seen from the comparison of Figs. 1 and 2. From Fig. 2 it also follows that, as in the case of the $n=2$ flexural shell modes, acoustic excitation of the $n=3$ mode results in the upward shift of the upper edge of the corresponding quasi-band-gap (transmission minimum in complete cylinder SCs). Therefore, the transmission peaks observed at the pseudogap of the SC are always accompanied by the widening of that pseudogap. Moreover, this widening increases with increasing filling fraction of the thin-walled hollow cylinders in the SC.

In conclusion, theoretical evidence for Fano-like resonance phenomena due to flexural shell vibration modes in transmission properties of phononic crystals made of 2D arrays of thin-walled hollow cylinders in air has been presented. It has been demonstrated by our analysis and simulations that high transmission of sound through the shell at flexural mode frequencies is a must for resonance excitation of these modes. An analytical formula has also been provided for the frequencies of these flexural shell modes, which can be used for the tuning of the acoustic properties of phononic crystals. Two-dimensional composite media with these internal modes are possible candidates for the design of metamaterials based on sonic crystals. Our work provides an alternative method of sound control of airborne phononic crystals.

Yu.A.K. would like to thank L. I. Manevitch for useful discussions. This work was supported by Spanish Ministry of Science and Education under project TEC2004-03545. Yu.A.K. also acknowledges financial support from Generalitat Valenciana (Grant No. CTESIN/2005/022). C.G. acknowledges the support by the Walloon Region and the European funds ERDF and ESF under Contract No. EP1A122030000102.

*Permanent address: N. N. Semenov Institute of Chemical Physics, Russian Academy of Sciences, ul. Kosygina 4, 119991 Moscow, Russia. Email address: yukosevich@yahoo.com
†Email address: cecile.goffaux@cenaero.be
‡Email address: jsdehesa@upvnet.upv.es

[1] For a review, see the special issue of Z. Kristallogr. **220**, (2005).
[2] J. V. Sánchez-Perez, D. Caballero, R. Mártinez-Sala, C. Rubio, J. Sánchez-Dehesa, F. Meseguer, J. Llinares, and F. Gálvez, Phys. Rev. Lett. **80**, 5325 (1998).
[3] F. Cervera, L. Sanchis, J. V. Sánchez-Perez, R. Mártinez-Sala, C. Rubio, F. Meseguer, C. López, D. Caballero, and J. Sánchez-Dehesa, Phys. Rev. Lett. **88**, 023902 (2002).
[4] A. A. Krokhin, J. Arriaga and L. N. Gumen, Phys. Rev. Lett. **91**, 264302 (2003).
[5] D. Torrent, A. Håkansson, F. Cervera, and J. Sánchez-Dehesa, Phys. Rev. Lett. **96**, 204302 (2006).
[6] A. Leissa, *Vibration of Shells* (Acoustic Society of America, New York, 1993).
[7] A. I. Manevich and L. I. Manevitch, *The Mechanics of Nonlinear Systems with Internal Resonances* (Imperial College Press, London, 2005).
[8] U. Fano, Phys. Rev. **124**, 1866 (1961).
[9] Yu. A. Kosevich, Prog. Surf. Sci. **55**, 1 (1997).
[10] Zh. Liu, X. Zhang, Y. Mao, Y. Y. Zhu, Zh. Yang, C. T. Chan, and P. Sheng, Science **289**, 1734 (2000).
[11] C. Goffaux, J. Sánchez-Dehesa, A. L. Yeyati, Ph. Lambin, A. Khelif, J. O. Vasseur, and B. Djafari-Rouhani, Phys. Rev. Lett. **88**, 225502 (2002).
[12] C. Goffaux and J. Sánchez-Dehesa, Phys. Rev. B **67**, 144301 (2003); **72**, 099903(E) (2005).
[13] K. Saijyou and S. Yoshikawa, J. Acoust. Soc. Am. **112**, 2808 (2002).
[14] D. H. Towne, *Wave Phenomena* (Dover, New York, 1988).
[15] A. Khelif, P. A. Deymier, B. Djafari-Rouhani, J. O. Vasseur, and L. Dobrzynski, J. Appl. Phys. **94**, 1308 (2003).
[16] Y. Pennec, B. Djafari-Rouhani, J. O. Vasseur, A. Khelif, and P. A. Deymier, Phys. Rev. E **69**, 046608 (2004).